Supplement of

Particle-associated benzotriazole ultraviolet stabilizers exhibit atmospheric persistence against ·OH heterogeneous oxidation

Kang Gao[1], Liuqing Zhao[2], Guangli Xiu[1], Xinke Wang[3], Lei Zhou[1*]

[1]State Environmental Protection Key Lab of Environmental Risk Assessment and Control on Chemical Processes, School of Resources and Environmental Engineering, East China University of Science and Technology, Shanghai 200237, China
[2]SCIEX Analytical Instrument Trading Co., Ltd, Shanghai 200000, China
[3]Shanghai Key Laboratory of Atmospheric Particle Pollution and Prevention (LAP3), National Observations and Research Station for Wetland Ecosystems of the Yangtze Estuary, Department of Environmental Science and Engineering, Fudan University, Shanghai 200438, China

Correspondence to: Lei Zhou (zhoulei@ecust.edu.cn)

Text S1. Oxidation Flow Tube

The photochemical oxidation flow tube (OFR) was equipped with a quartz window for UV irradiation, and an outer jacket for circulating water. The volume of OFR was determined to be 4.0 L, and the light intensity in the OFR was 2.0 mW cm^{-2}. An internal sensor (Huakong, Model HSTL-F107) was employed for monitoring the temperature and relative humidity (RH) in the OFR. A methanol solution containing water (8:2, v/v) was used for particle collection with a sampling time of 30 min for each trial, and the extract was diluted to original volume after collection. For aerosol analysis, the sheath flow rate of SMPS (TSI, Model 3938) was 3.0 L min^{-1}, the size of impactor was 0.071 cm, and the scanning size range was 20–400 nm. For gas analysis, the flow rate of O_3 analyzer (Thermo Scientific, Model 49i) was 1.5 L min^{-1}, and of SO_2 analyzer (Thermo Scientific, Model 43i) was 0.5 L min^{-1}.

Text S2. Coating Film

Thin films were created on an optical coverslip (diameter = 15 mm) following literature procedures (Huang et al., 2026). Assuming an injection volume of 9.5 μL (BT-UVs dissolved in HPLC-grade acetone), the deposited BT-UVs film (density of 1.2 g cm^{-3}) is assumed to be uniform with a thickness of 10 nm:

$$V_{film} = \pi \times r^2 \times h = 1.77 \times 10^{-6}\ cm^3 \quad (1)$$

$$Mass = \rho \times V_{film} = 2.12 \times 10^{-6}\ g \quad (2)$$

$$C = Mass \div V_{inject} = 223\ mg\ L^{-1} \quad (3)$$

Text S3. Quantitative Analysis

An ACQUITY Premier BEH C18 column (1.7 μm, 100 × 2.1 mm) was employed for chromatographic separation. The mobile phase contained solvent A (0.1% formic acid in ultra-pure water) and solvent B (10 mmol L^{-1} ammonium acetate in methanol). A gradient elution program was performed at a flow rate of 0.35 mL min^{-1}: initially 70% B held for 1.0 min, linearly increased to 95% B over 2.0 min and maintained for 4.0 min, then linearly returned to 70% B within 0.1 min and equilibrated for 0.9 min. The injection volume was 5.0 μL, and the column temperature was set at 45 °C.

An electrospray ionization (ESI^+) was employed. The ion source gas 1 (GS1) was 45 psi, ion source gas 2 (GS2) was 45 psi, curtain gas (CUR) was 35 psi, entrance potential (EP) was 10 V, ion source temperature (TEM) was 500 °C, and ion spray voltage (IS) was 5500 V.

Text S4. Suspect Screening

A Kinetex® C18 column (2.6 μm, 100 × 2.1 mm) was employed for the chromatographic separation. The mobile phase contained solvent A (0.1% formic acid in ultra-pure water) and solvent B (10 mmol L^{-1} ammonium acetate in methanol). A gradient elution program was performed at a flow rate of 0.35 mL min^{-1}: initially 30% B held for 1.0 min, linearly increased to 95% B over 2.0 min and maintained for 5.0 min, then linearly increased to 100% B over 1.0 min, and maintained for 7.0 min, followed by linearly decreased to 30% B within 0.1 min and equilibrated for 0.9 min. The injection volume was 5.0 μL, and the column temperature was set at 45 °C.

A Turbo V™ electrospray ionization was employed. The GS1 was 55 psi, GS2 was 55 psi, CUR was 35 psi, TEM was 500 °C, IS was 5500 V, and collision gas (CAD) was 7 psi. For MS^1 scanning, the mass ranges were set from 50 to 1000 m/z, DP was 80 V and CE was 10 eV. For MS^2 scanning, the mass ranges were set from 30 to 1000 m/z, DP was 80 V, CE was 35 eV, and collision energy spread (CES) was 15 eV.

Text S5. Quality Control and Quality Assurance

The collection efficiencies of BT-UVs in the collection trap were determined to be greater than 80% by quantifying the mass loss of BT-UVs upon heating their corresponding concentrations in the extractant. The matrix spike recoveries and relative standard deviations (RSDs) of BT-UVs in filters were ranged from 72 ± 4.2% to 83 ± 5.8% across three spiked levels (1 μg kg^{-1}, 10 μg kg^{-1}, 100 μg kg^{-1}). The method detection limit (MDL) was defined as three times the signal-to-noise (S/N) ratio obtained for standards prepared in the matrix at the lowest detectable concentration. The limit of quantification (LOQ) was defined as the lowest spiked level of the validation meeting the method performance acceptability criteria. For instrumental analysis, one

procedural blank and one replicate sample were analyzed alongside every batch of five samples, and the relative standard deviations of replicate samples were all below 10%.

Table S1. Information on name, CAS No., formula, molecular weight (M_w), saturated vapor pressure (SVP), log K_{ow}, and log K_{oa} of each BT-UV.

BT-UVs	CAS No.	Formula	M_w (g mol^{-1})	SVP (pa)	log K_{ow}	log K_{oa}
UV-P	2440-22-4	$C_{13}H_{11}N_3O$	225.25	2.72×10^{-5}	4.3	9.8
UV-234	70321-86-7	$C_{30}H_{29}N_3O$	447.57	4.90×10^{-7}	6.5	17.1
UV-326	3896-11-5	$C_{17}H_{18}ClN_3O$	315.80	7.59×10^{-7}	5.6	11.0
UV-327	3864-99-1	$C_{20}H_{24}ClN_3O$	357.88	3.72×10^{-6}	6.9	10.6
UV-328	25973-55-1	$C_{22}H_{29}N_3O$	351.49	9.77×10^{-5}	6.5	10.5
UV-329	3147-75-9	$C_{20}H_{25}N_3O$	323.43	4.17×10^{-6}	6.2	10.8
UV-360	103597-45-1	$C_{41}H_{50}N_6O_2$	658.87	4.17×10^{-6}	9.0	25.2
UV-928	73936-91-1	$C_{29}H_{35}N_3O$	441.61	3.98×10^{-7}	8.8	16.7

Table S2. List of $^{\bullet}$OH oxidation experiments under different conditions, and the corresponding model results under those conditions.

RH	#	SO_2 Initial (ppb)	OHR (s^{-1})	SO_2 Final (ppb)	O_3 Final (ppb)	$^{\bullet}OH_{exp}$ (molecules cm^{-3} s)
25%	Con.1	1148.0	25.4	840.7	9234.9	3.5×10^{11}
	Con.2	1127.2	25.0	760.9	10169.2	4.4×10^{11}
	Con.3	1131.7	25.1	685.1	12881.3	5.6×10^{11}
	Con.4	1092.6	24.0	602.5	17003.3	6.6×10^{11}
50%	Con.1	1105.4	24.5	762.6	6387.9	4.1×10^{11}
	Con.2	1078.6	23.9	647.8	9829.0	5.7×10^{11}
	Con.3	1134.4	25.1	569.5	10956.1	7.7×10^{11}
	Con.4	1121.7	24.8	502.0	12724.2	8.9×10^{11}

Table S3. Optimized MRM parameters for BT-UVs.

BT-UVs	Adduct/Charge	Precursor Ion (m/z)	Qualifier Ion (m/z)	Declustering Potential (V)	Collision Energy (eV)
UV-P	[M+H]+	226.1	107.0/120.1	50.0	26.0/25.0
UV-234	[M+H]+	448.3	119.1/370.2	50.0	45.0/27.0
UV-326	[M+H]+	316.1	132.1/260.0	50.0	40.0/27.0
UV-327	[M+H]+	358.3	302.0/340.5	50.0	31.0/37.0
UV-328	[M+H]+	352.2	140.1/282.2	50.0	29.0/33.0
UV-329	[M+H]+	324.2	140.1/212.2	50.0	27.0/33.0
UV-360	[M+H]+	659.4	301.1/336.2	50.0	25.0/40.0
UV-928	[M+H]+	442.3	252.2/364.2	50.0	47.0/31.0

Table S4. Second-order rate constants (k) and ˙OH reactive uptake coefficients (γ) for particle-associated BT-UVs.

BT-UVs	k_{obs} (cm^3 $molecules^{-1}$ s^{-1})	γ_{obs}	k_{exp} (cm^3 $molecules^{-1}$ s^{-1})	γ_{exp}
UV-P	$(4.05 \pm 0.29) \times 10^{-13}$	$(7.29 \pm 0.52) \times 10^{-2}$	$(4.12 \pm 0.30) \times 10^{-13}$	$(7.41 \pm 0.53) \times 10^{-2}$
UV-234	$(11.6 \pm 0.73) \times 10^{-13}$	$(8.77 \pm 0.55) \times 10^{-2}$	$(11.9 \pm 0.75) \times 10^{-13}$	$(8.93 \pm 0.56) \times 10^{-2}$
UV-326	$(8.58 \pm 0.88) \times 10^{-13}$	$(10.6 \pm 1.09) \times 10^{-2}$	$(8.80 \pm 0.90) \times 10^{-13}$	$(10.8 \pm 1.11) \times 10^{-2}$
UV-327	$(9.38 \pm 0.49) \times 10^{-13}$	$(9.73 \pm 0.51) \times 10^{-2}$	$(9.64 \pm 0.50) \times 10^{-13}$	$(9.91 \pm 0.52) \times 10^{-2}$
UV-328	$(9.73 \pm 0.63) \times 10^{-13}$	$(8.80 \pm 0.57) \times 10^{-2}$	$(10.0 \pm 0.65) \times 10^{-13}$	$(8.96 \pm 0.58) \times 10^{-2}$
UV-329	$(12.3 \pm 0.48) \times 10^{-13}$	$(13.3 \pm 0.52) \times 10^{-2}$	$(12.8 \pm 0.50) \times 10^{-13}$	$(13.5 \pm 0.53) \times 10^{-2}$
UV-360	$(12.9 \pm 1.15) \times 10^{-13}$	$(6.89 \pm 0.52) \times 10^{-2}$	$(13.2 \pm 1.17) \times 10^{-13}$	$(7.01 \pm 0.63) \times 10^{-2}$
UV-928	$(11.5 \pm 1.01) \times 10^{-13}$	$(8.81 \pm 0.78) \times 10^{-2}$	$(11.8 \pm 1.04) \times 10^{-13}$	$(8.97 \pm 0.79) \times 10^{-2}$

Table S5. Second-order rate constants (k) and atmospheric lifetimes (τ) for BT-UVs in the gas and particle phases.

BT-UVs	k_{exp} (cm^3 $molecules^{-1}$ s^{-1})	k_{AOPWIN} (cm^3 $molecules^{-1}$ s^{-1})	τ_{exp} (days)	τ_{AOPWIN} (days)
UV-P	$(4.12 \pm 0.30) \times 10^{-13}$	3.05×10^{-11}	30 ± 10	0.41 ± 0.54
UV-234	$(11.9 \pm 0.75) \times 10^{-13}$	2.17×10^{-11}	11 ± 3.6	0.58 ± 0.20
UV-326	$(8.80 \pm 0.90) \times 10^{-13}$	1.49×10^{-11}	14 ± 4.9	0.84 ± 0.29
UV-327	$(9.64 \pm 0.50) \times 10^{-13}$	1.32×10^{-11}	13 ± 4.5	0.95 ± 0.33
UV-328	$(10.0 \pm 0.65) \times 10^{-13}$	1.58×10^{-11}	13 ± 4.3	0.79 ± 0.27
UV-329	$(12.8 \pm 0.50) \times 10^{-13}$	3.20×10^{-11}	9.8 ± 3.4	0.39 ± 0.13
UV-360	$(13.2 \pm 1.17) \times 10^{-13}$	3.32×10^{-11}	9.5 ± 3.3	0.38 ± 0.13
UV-928	$(11.8 \pm 1.04) \times 10^{-13}$	1.93×10^{-11}	11 ± 3.7	0.65 ± 0.22

Table S6. Atmospheric half-lives ($t_{1/2}$), overall persistence (P_{OV}), characteristic travel distance (CTD) and remotely transferred fraction ($\varphi 2$) for BT-UVs.

BT-UVs	$t_{1/2}$ (hours)	P_{OV} (days)	CTD (km)	$\varphi 2$
UV-P	4.09×10^2	1.08×10^2	1.43×10^3	6.03×10^{-4}
UV-234	1.42×10^2	1.73×10^2	2.86×10^3	1.41×10^{-3}
UV-326	1.92×10^2	1.73×10^2	1.72×10^3	6.68×10^{-4}
UV-327	1.75×10^2	1.73×10^2	2.26×10^3	6.00×10^{-4}
UV-328	1.69×10^2	1.73×10^2	2.09×10^3	5.56×10^{-4}
UV-329	1.32×10^2	1.73×10^2	1.84×10^3	5.23×10^{-4}
UV-360	1.28×10^2	5.19×10^2	2.86×10^3	1.40×10^{-3}
UV-928	1.43×10^2	5.19×10^2	2.86×10^3	1.40×10^{-3}

Table S7. Atmospheric half-lives ($t_{1/2}$), overall persistence (P_{OV}), characteristic travel distance (CTD) and remotely transferred fraction (φ2) of reference POPs from the OECD database.

POPs	$t_{1/2}$ (hours)	P_{OV} (days)	CTD (km)	φ2
BDE-169	1.10×10^3	1.82×10^3	2.90×10^3	1.44×10^{-3}
BDE-193	1.60×10^3	2.77×10^3	2.86×10^3	1.42×10^{-3}
BDE-209	7.61×10^3	9.48×10^2	2.87×10^3	1.42×10^{-3}
BDE-47	3.84×10^2	5.65×10^2	3.29×10^3	1.12×10^{-3}
BDE-99	3.60×10^2	2.16×10^2	2.86×10^3	1.23×10^{-3}
beta-HCH	1.34×10^3	2.52×10^3	4.02×10^3	2.99×10^{-3}
chlordecone	1.00×10^{10}	1.06×10^3	1.66×10^3	1.38×10^{-3}
chlorpyrifos	9.05	39.3	1.82×10^2	3.04×10^{-5}
dechlorane plus	13.7	5.19×10^2	1.82×10^3	5.51×10^{-4}
dicofol	93.6	1.75×10^2	1.26×10^3	2.79×10^{-4}
gamma-HCH	1.34×10^3	2.10×10^2	3.59×10^3	1.51×10^{-3}
HBCD	31.2	1.22×10^2	5.91×10^2	7.56×10^{-5}
HCBD	8.76×10^3	3.49×10^2	8.64×10^4	1.90×10^{-2}
hexabromobiphenyl	3.18×10^3	3.57×10^2	4.16×10^3	2.02×10^{-3}
MCCPs (C14)	54.3	5.03×10^2	1.11×10^3	4.18×10^{-5}
methoxychlor	4.80	1.73×10^2	1.14×10^2	4.80×10^{-5}
pentachlorobenzene	3.72×10^3	7.14×10^2	6.70×10^4	2.67×10^{-3}
SCCPs (C10)	1.44×10^2	5.12×10^2	2.07×10^3	3.58×10^{-4}
tech-endosulfan	3.60×10^2	1.52×10^2	3.82×10^3	9.44×10^{-4}
tri-PCN	1.92×10^2	3.23×10^2	3.71×10^3	1.24×10^{-4}

Table S8. Second-order rate constants (*k*) for particle-associated BT-UVs in different conditions.

BT-UVs	k_{exp} (cm^3 $molecules^{-1}$ s^{-1})			
	AS at 25% RH	AS at 50% RH	FS at 25% RH	FS at 50% RH
UV-P	$(4.12 \pm 0.30) \times 10^{-13}$	$(7.77 \pm 0.47) \times 10^{-13}$	$(5.43 \pm 0.42) \times 10^{-13}$	$(7.92 \pm 0.52) \times 10^{-13}$
UV-234	$(11.9 \pm 0.75) \times 10^{-13}$	$(14.8 \pm 1.13) \times 10^{-13}$	$(13.5 \pm 1.66) \times 10^{-13}$	$(15.7 \pm 1.99) \times 10^{-13}$
UV-326	$(8.80 \pm 0.90) \times 10^{-13}$	$(10.9 \pm 0.29) \times 10^{-13}$	$(9.80 \pm 0.31) \times 10^{-13}$	$(12.3 \pm 0.79) \times 10^{-13}$
UV-327	$(9.64 \pm 0.50) \times 10^{-13}$	$(10.4 \pm 0.95) \times 10^{-13}$	$(9.73 \pm 0.26) \times 10^{-13}$	$(12.1 \pm 0.55) \times 10^{-13}$
UV-328	$(10.0 \pm 0.65) \times 10^{-13}$	$(10.9 \pm 0.72) \times 10^{-13}$	$(10.1 \pm 0.61) \times 10^{-13}$	$(11.2 \pm 0.29) \times 10^{-13}$
UV-329	$(12.8 \pm 0.50) \times 10^{-13}$	$(14.4 \pm 0.42) \times 10^{-13}$	$(13.2 \pm 0.51) \times 10^{-13}$	$(15.4 \pm 0.69) \times 10^{-13}$
UV-360	$(13.2 \pm 1.17) \times 10^{-13}$	$(13.6 \pm 1.15) \times 10^{-13}$	$(12.9 \pm 1.88) \times 10^{-13}$	$(14.3 \pm 1.03) \times 10^{-13}$
UV-928	$(11.8 \pm 1.04) \times 10^{-13}$	$(14.9 \pm 0.25) \times 10^{-13}$	$(12.3 \pm 1.72) \times 10^{-13}$	$(16.4 \pm 0.65) \times 10^{-13}$

Table S9. Atmospheric lifetimes (τ) for particle-associated BT-UVs in different conditions.

BT-UVs	τ (days)			
	AS at 25% RH	AS at 50% RH	FS at 25% RH	FS at 50% RH
UV-P	30 ± 10	16 ± 5.6	23 ± 7.9	16 ± 5.4
UV-234	11 ± 3.6	8.5 ± 2.9	9.3 ± 3.2	8.0 ± 2.7
UV-326	14 ± 4.9	11 ± 3.9	13 ± 4.4	10 ± 3.5
UV-327	13 ± 4.5	12 ± 4.2	13 ± 4.5	10 ± 3.6
UV-328	13 ± 4.3	11 ± 3.9	12 ± 4.3	11 ± 3.9
UV-329	9.8 ± 3.4	8.7 ± 3.1	9.5 ± 3.3	8.1 ± 2.8
UV-360	9.5 ± 3.3	9.2 ± 3.2	9.7 ± 3.1	8.8 ± 3.0
UV-928	11 ± 3.7	8.4 ± 2.9	10 ± 3.6	7.6 ± 2.6

Table S10. Detailed information of suspected TPs.

Precursor	ID	Formula	Exact mass	Mass error	R.T. (min)	Putative structure

				(ppm)		
UV-P	TP260	$C_{13}H_{13}N_3O_3$	260.1030	0.0	4.1	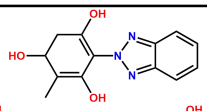
UV-P	TP258	$C_{13}H_{11}N_3O_3$	258.0873	0.4	4.1/4.4	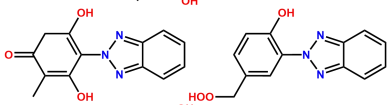
UV-P	TP256	$C_{13}H_9N_3O_3$	256.0717	–0.4	4.4	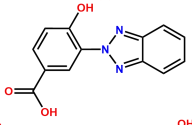
UV-P	TP242	$C_{13}H_{11}N_3O_2$	242.0924	–0.4	4.1	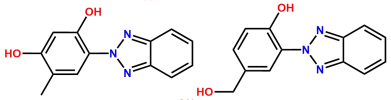
UV-P	TP240	$C_{13}H_9N_3O_2$	240.0768	0.8	4.5	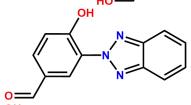
UV-234	TP486	$C_{28}H_{27}N_3O_5$	486.2024	1.0	6.2	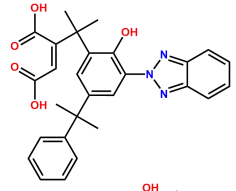
UV-234	TP470	$C_{28}H_{27}N_3O_4$	470.2074	–0.4	4.3/6.6	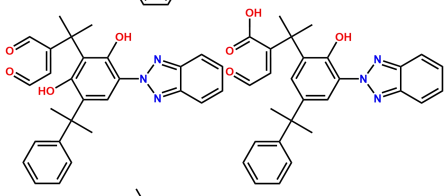
UV-326	TP348	$C_{17}H_{18}ClN_3O_3$	348.1109	1.1	4.5	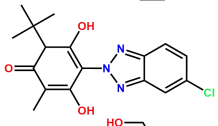
UV-326	TP332	$C_{17}H_{18}ClN_3O_2$	332.1160	0.3	4.5/4.8	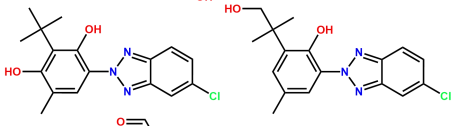
UV-326	TP330	$C_{17}H_{16}ClN_3O_2$	330.1004	2.7	4.6	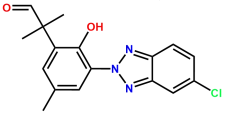
UV-326	TP276	$C_{13}H_{10}ClN_3O_2$	276.0534	2.5	4.5	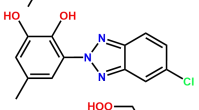
UV-327	TP390	$C_{20}H_{24}ClN_3O_3$	390.1579	2.3	4.7/5.0	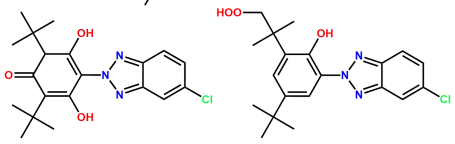

UV-327	TP374	$C_{20}H_{24}ClN_3O_2$	374.1629	2.4	4.7/5.0	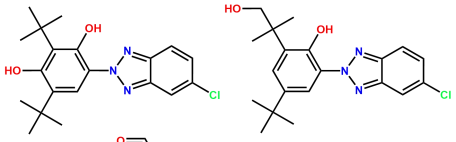
UV-327	TP372	$C_{20}H_{22}ClN_3O_2$	372.1473	2.1	4.8	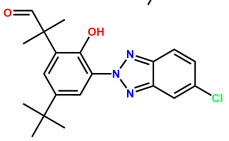
UV-327	TP318	$C_{16}H_{16}ClN_3O_2$	318.1004	2.5	4.7	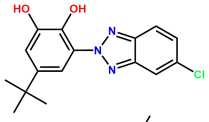
UV-328	TP384	$C_{22}H_{29}N_3O_3$	384.2282	1.8	4.6/5.0	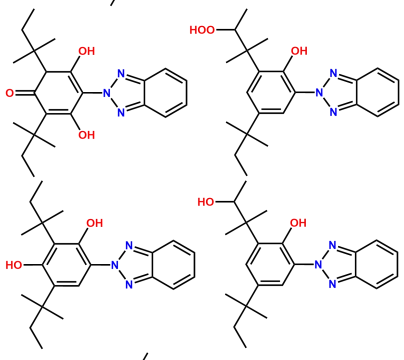
UV-328	TP368	$C_{22}H_{29}N_3O_2$	368.2333	0.5	4.6/5.0	
UV-328	TP366	$C_{22}H_{27}N_3O_2$	366.2176	0.0	4.9	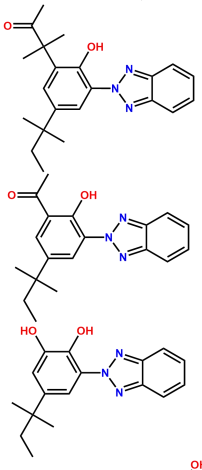
UV-328	TP324(1)	$C_{19}H_{21}N_3O_2$	324.1707	1.9	4.8	
UV-328	TP298	$C_{17}H_{19}N_3O_2$	298.1550	1.0	4.6	
UV-329	TP356	$C_{20}H_{25}N_3O_3$	356.1969	–1.1	4.6/4.7	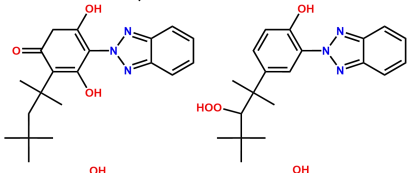
UV-329	TP340	$C_{20}H_{25}N_3O_2$	340.2019	0.6	4.7	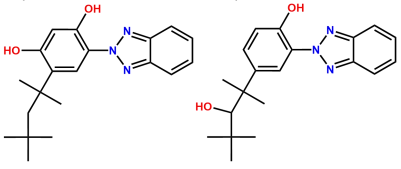

UV-329	TP338	$C_{20}H_{23}N_3O_2$	338.1863	3.0	4.9	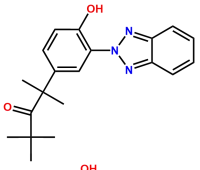
UV-329	TP254	$C_{14}H_{11}N_3O_2$	254.0924	2.8	4.5	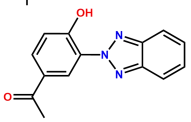
UV-360	TP687	$C_{41}H_{46}N_6O_4$	687.3653	1.0	4.6/4.8	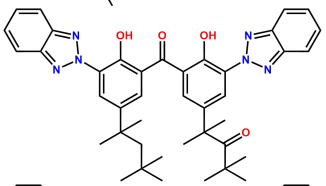
UV-360	TP675	$C_{41}H_{50}N_6O_3$	675.4017	1.5	4.8/5.4	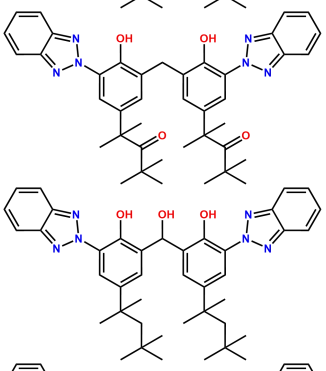
UV-360	TP-324(2)	$C_{20}H_{25}N_3O$	324.2070	0.0	5.5	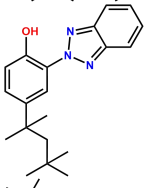
UV-928	TP480	$C_{27}H_{33}N_3O_5$	480.2493	0.0	7.2	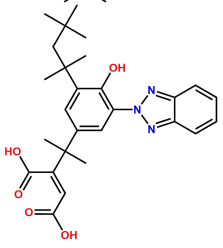

UV-928	TP476	$C_{29}H_{37}N_3O_3$	476.2908	0.4	4.0	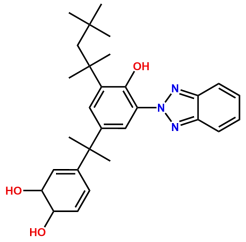
UV-928	TP474	$C_{29}H_{35}N_3O_3$	474.2751	0.0	4.4/5.2	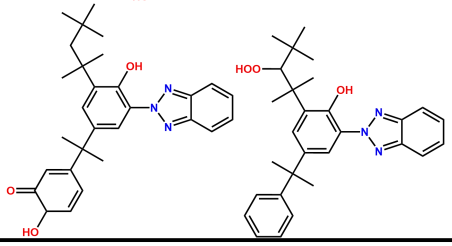

Table S11. Concentrations (pg m^{-3}) of BT-UVs in Shanghai's $PM_{2.5}$.

Sampling date	UV-P	UV-234	UV-326	UV-327	UV-328	UV-329	UV-360	UV-928	Total
19/11/2025	9.5	4.7	18	6.0	1.9	3.1	12	1.2	57
20/11/2025	3.5	2.7	20	3.9	10	3.3	4.2	/	48
21/11/2025	4.8	2.9	20	5.5	1.5	5	6.3	/	47
22/11/2025	6.2	12	60	3.1	2.9	55	7.1	1.3	1.5×10^2
23/11/2025	7.5	12	55	3.0	13	18	8.5	2.5	1.2×10^2
24/11/2025	10	1.4×10^2	26	2.4	2.0	49	4.9	1.0	2.4×10^2
25/11/2025	7.5	2.6	15	5.0	4.7	1.1×10^2	3.3	/	1.5×10^2
26/11/2025	11	2.4	25	5.3	3.6	8	5.2	/	61
27/11/2025	4.3	2.7	18	2.5	14	5	4.2	1.2	52

Table S12. Predicted no-effect concentration (PNEC) and toxicity variation coefficient (TVC) for BT-UVs and TPs.

Precursor	Compound ID	Pred_Value: –Log10 (mol kg^{-1})	Pred _Value: mg kg^{-1}	PNEC_Value: μg kg^{-1}	TVC
/	UV-P	2.50	719.6	719.6	0
UV-P	TP260	2.55	733.9	733.9	–0.02
UV-P	TP258	2.57	689.0	689.0	0.04
UV-P	TP256	2.71	498.0	498.0	0.44
UV-P	TP242	2.50	770.1	770.1	–0.07
UV-P	TP240	2.76	414.2	414.2	0.74
/	UV-234	2.63	1041.0	1041.0	0
UV-234	TP486	3.38	200.4	200.4	4.19
UV-234	TP470	3.07	397.3	397.3	1.62
/	UV-326	2.19	2052.2	2052.2	0
UV-326	TP348	2.37	1470.0	1470.0	0.40
UV-326	TP332	2.22	2022.5	2022.5	0.01
UV-326	TP330	2.23	1920.9	1920.9	0.07
UV-326	TP276	2.38	1146.5	1146.5	0.79
/	UV-327	2.21	2209.9	2209.9	0
UV-327	TP390	2.68	818.3	818.3	1.70
UV-327	TP374	2.25	2105.3	2105.3	0.05
UV-327	TP372	2.20	2324.6	2324.6	–0.05
UV-327	TP318	2.45	1128.0	1128.0	0.96
/	UV-328	2.46	1232.3	1232.3	0
UV-328	TP384	2.57	1031.8	1031.8	0.19
UV-328	TP368	2.43	1372.8	1372.8	–0.10
UV-328	TP366	2.45	1289.1	1289.1	–0.04

UV-328	TP324	2.21	2010.7	2010.7	–0.39
UV-328	TP298	2.49	960.1	960.1	0.28
/	UV-329	2.03	2989.0	2989.0	0
UV-329	TP356	2.32	1684.9	1684.9	0.77
UV-329	TP340	2.10	2727.4	2727.4	0.10
UV-329	TP338	2.09	2720.9	2720.9	0.10
UV-329	TP254	2.51	781.4	781.4	2.83
/	UV-360	3.15	471.9	471.9	0
UV-360	TP687	3.69	139.8	139.8	2.38
UV-360	TP675	3.14	483.4	483.4	–0.02
UV-360	TP324	2.03	2989.0	2989.0	–0.84
/	UV-928	2.28	2332.0	2332.0	0
UV-928	TP480	2.42	1807.3	1807.3	0.29
UV-928	TP476	2.40	1880.2	1880.2	0.24
UV-928	TP474	2.38	1970.2	1970.2	0.18

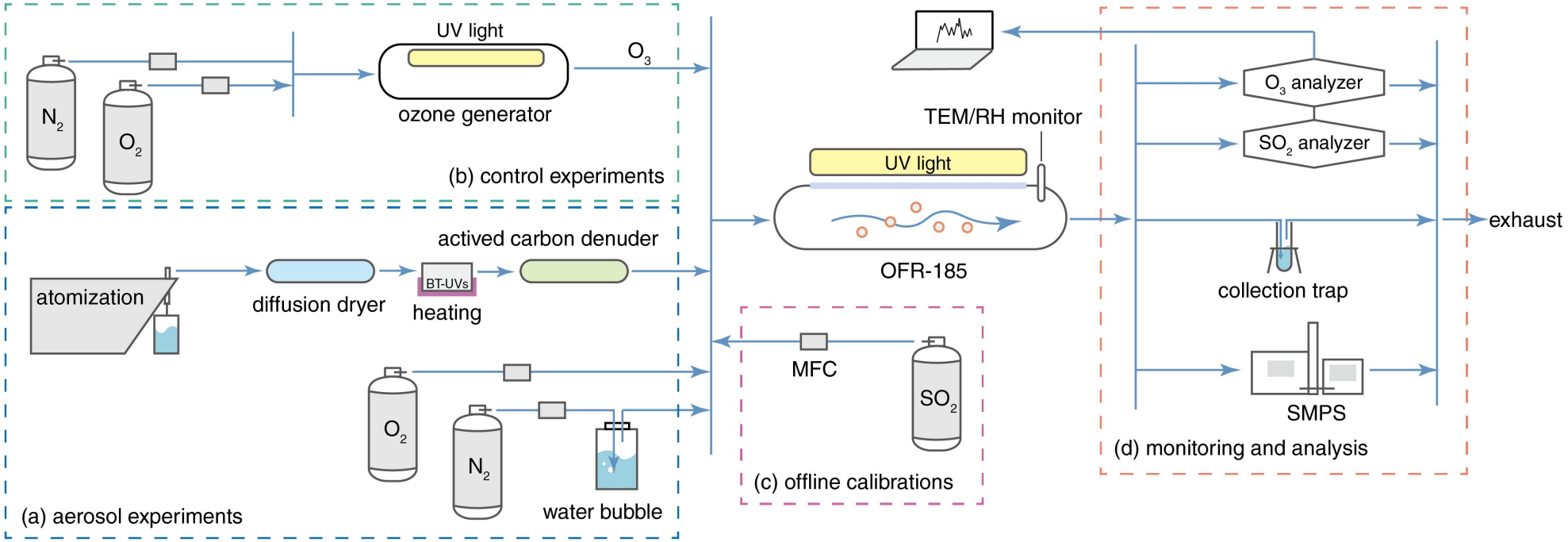

105 **Figure S1. Experimental setup for heterogeneous oxidation studies.**

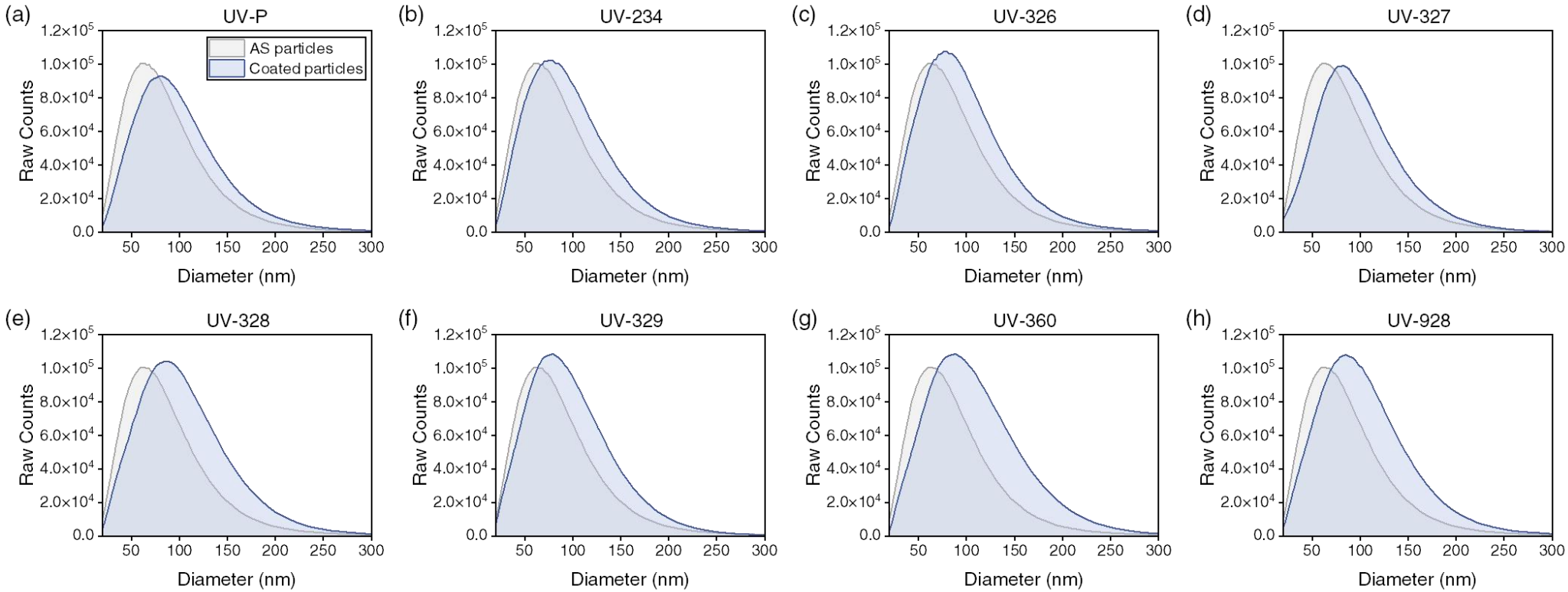

Figure S2. Diameters of AS particles and coated particles.

110

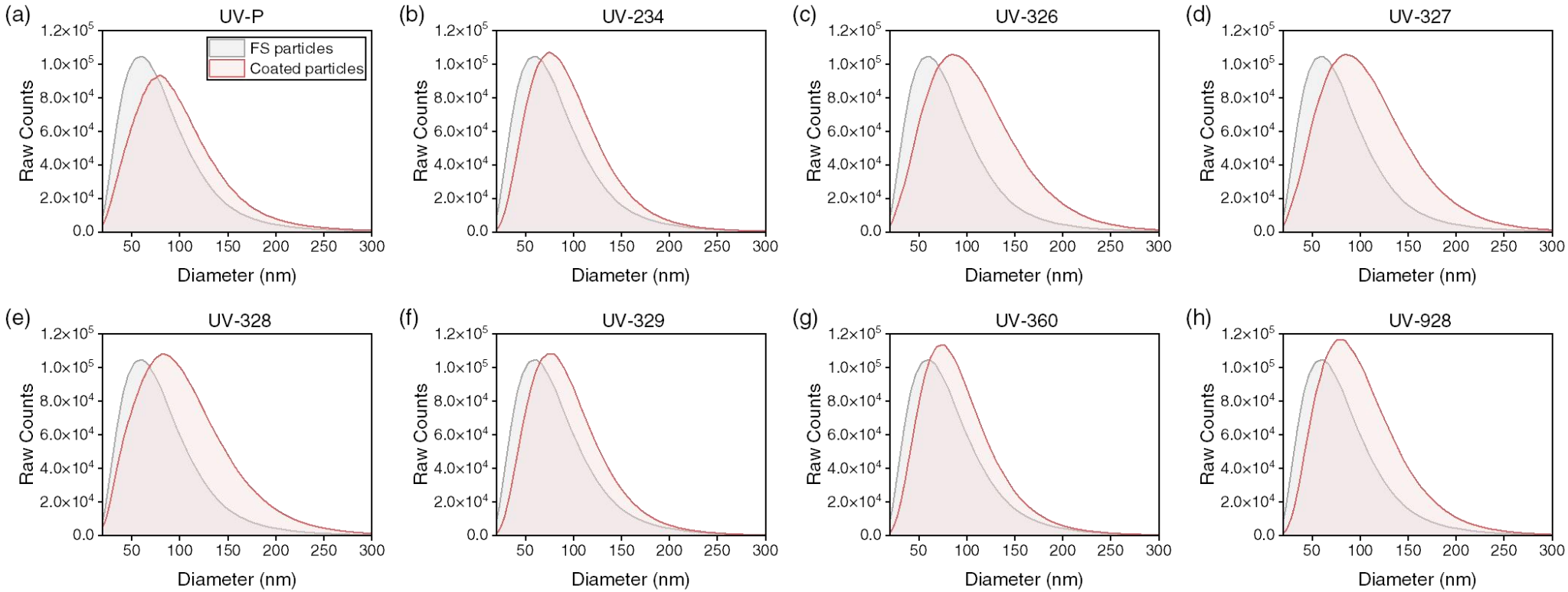

Figure S3. Diameters of FS particles and coated particles.

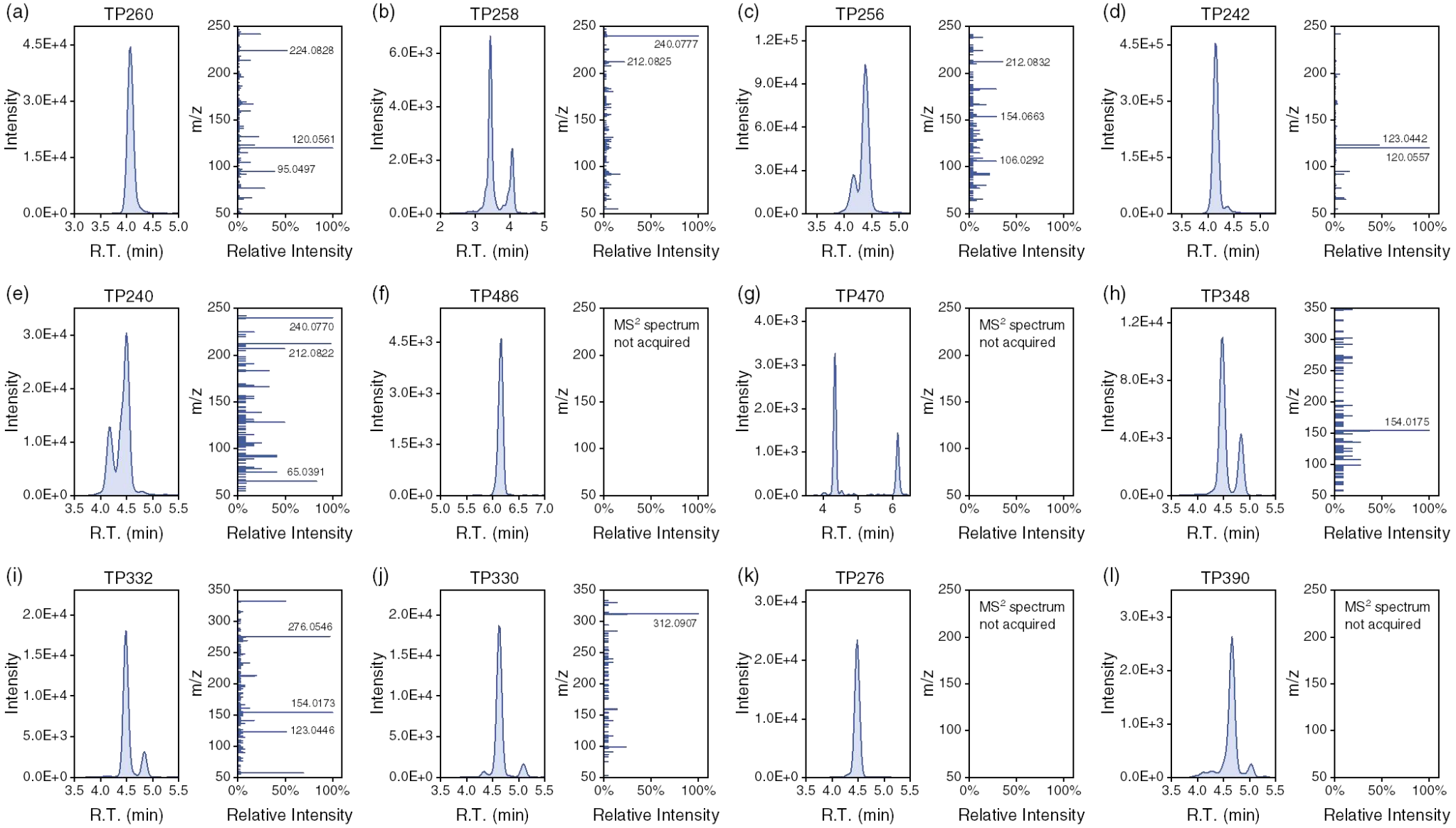

115

Figure S4. Extracted ion chromatogram (XIC) and MS^2 spectrum of TPs.

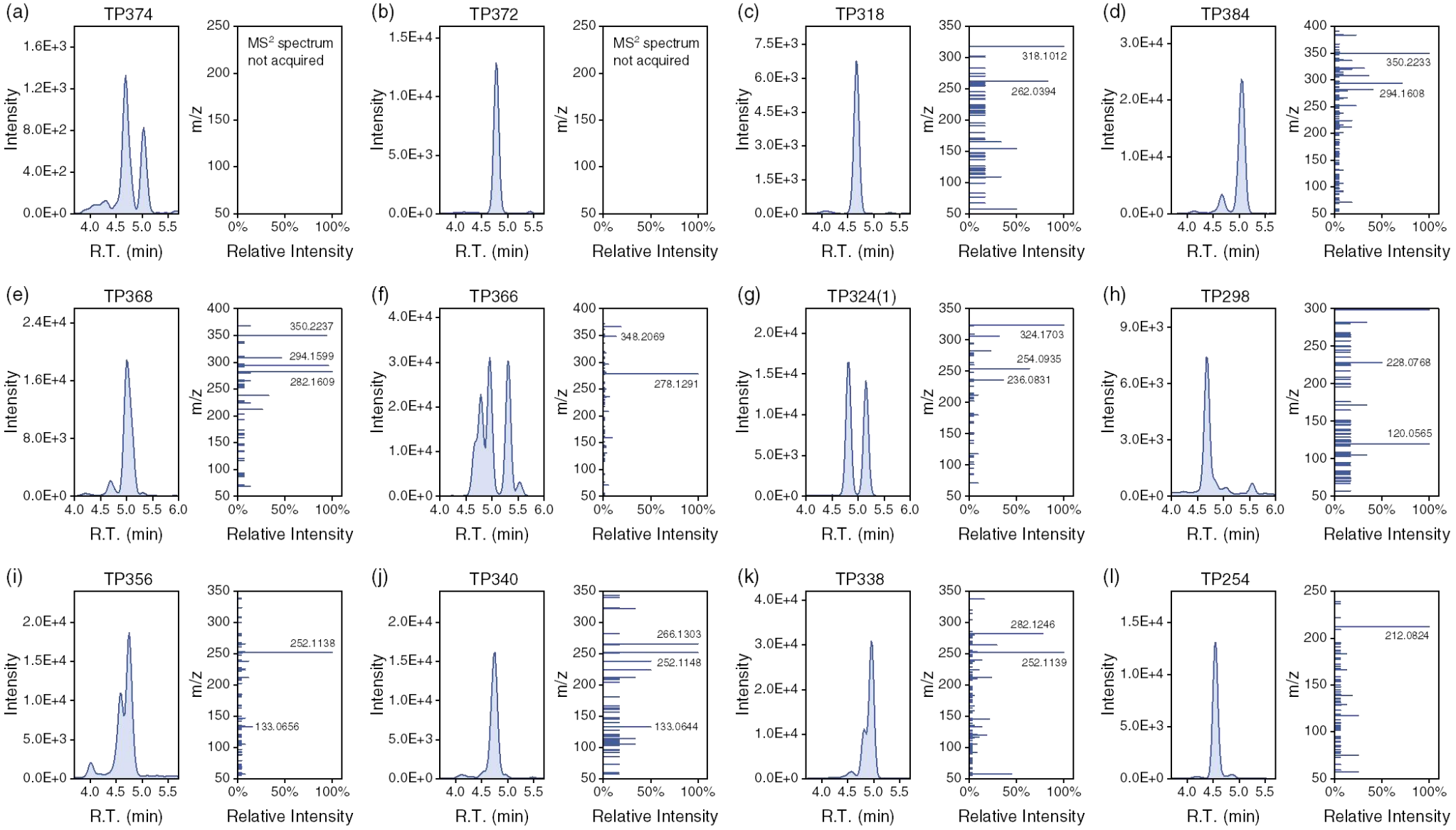

120 **Figure S5. Extracted ion chromatogram (XIC) and MS^2 spectrum of TPs.**

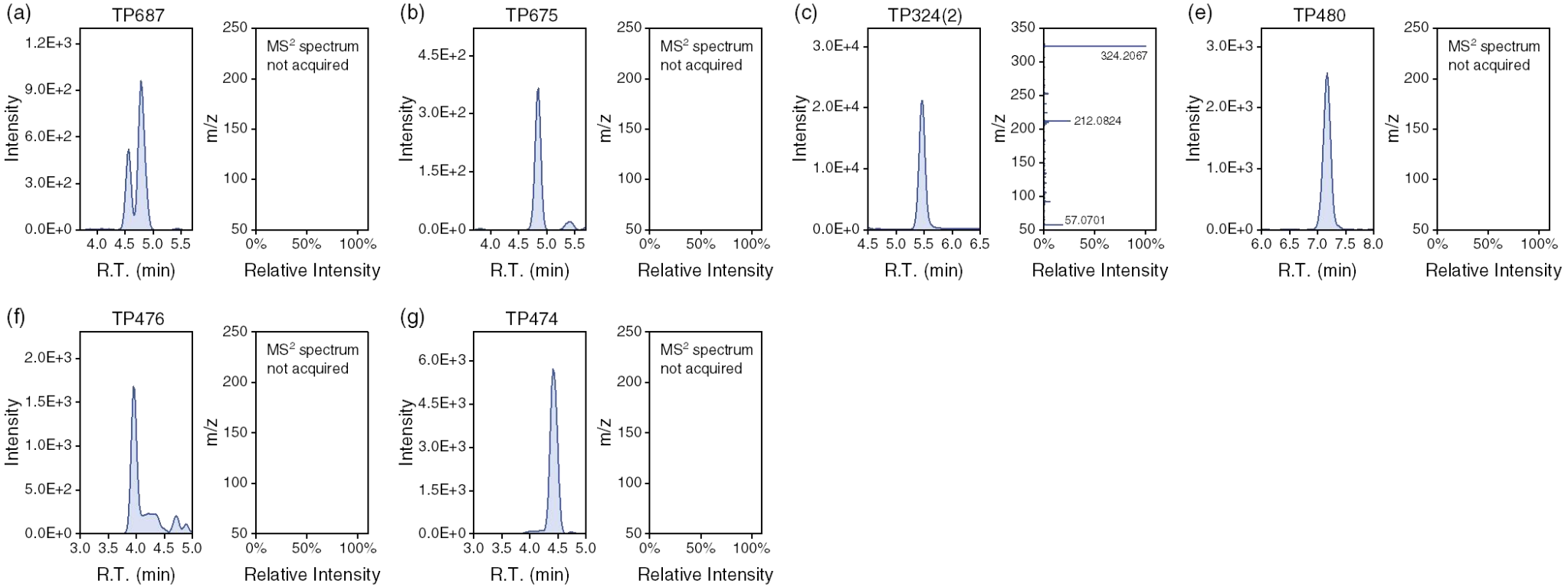

Figure S6. Extracted ion chromatogram (XIC) and MS^2 spectrum of TPs.

125

References

Huang, Y. Y., Wang, X., Xie, L., De Silva, A., Brinovcar, C., Peng, H., Wania, F., and Abbatt, J.: O3 and OH Multiphase Oxidation of Benzotriazole Ultraviolet Stabilizer UV-328, Environmental Science & Technology, 10.1021/acs.est.6c01932, 2026.